PHYSICAL REVIEW B **95**, 201305(R) (2017)

Limits to coherent scattering and photon coalescence from solid-state quantum emitters

Jake Iles-Smith,[1,2,*] Dara P. S. McCutcheon,[1,3] Jesper Mørk,[1] and Ahsan Nazir[2,†]

[1]*Department of Photonics Engineering, DTU Fotonik, Ørsteds Plads, 2800 Kongens Lyngby, Denmark*

[2]*Photon Science Institute & School of Physics and Astronomy, The University of Manchester, Oxford Road, Manchester M13 9PL, United Kingdom*

[3]*Quantum Engineering Technology Labs, H. H. Wills Physics Laboratory and Department of Electrical and Electronic Engineering, University of Bristol, BS8 1FD, United Kingdom*

(Received 24 June 2016; revised manuscript received 28 April 2017; published 25 May 2017)

The desire to produce high-quality single photons for applications in quantum information science has lead to renewed interest in exploring solid-state emitters in the weak excitation regime. Under these conditions it is expected that photons are coherently scattered, and so benefit from a substantial suppression of detrimental interactions between the source and its surrounding environment. Nevertheless, we demonstrate here that this reasoning is incomplete, as phonon interactions continue to play a crucial role in determining solid-state emission characteristics even for very weak excitation. We find that the sideband resulting from non-Markovian relaxation of the phonon environment is excitation strength independent. It thus leads to an intrinsic limit to the fraction of coherently scattered light and to the visibility of two-photon coalescence at weak driving, both of which are absent for atomic systems or within simpler Markovian treatments.

DOI: 10.1103/PhysRevB.95.201305

In the past few years, artificial atoms such as semiconductor quantum dots (QDs) have emerged as a leading platform to develop novel photonic sources for applications in quantum information science. This interest has been driven in part by a host of experiments establishing that QDs exhibit the optical properties of few-level systems, much as their natural atomic counterparts. This includes single photon emission and photon antibunching [1–6], entangled photon emission [7,8], coherent Rabi oscillations [9–11], and resonance fluorescence [12–20], which has culminated in recent demonstrations of efficiently generated, highly indistinguishable photons [21–24]. Moreover, the solid-state nature of QDs offers advantages not shared by atomic systems, such as the ease with which they can be optically addressed, larger oscillator strengths, and potential embedding into complex photonic structures [25,26]. However, less advantageous distinctions are also present, principally the unavoidable interactions between QD excitonic degrees of freedom and the environment provided by the host material [27–32]. These can significantly alter QD optical emission properties [33–36], which typically reduces performance in quantum photonic devices [37].

Recent efforts to suppress the detrimental effects of environmental coupling in solid-state emitters have renewed interest in studying the weak resonant excitation (Heitler) limit [13–19]. In atomic systems, this regime is dominated by elastic (coherent) scattering of photons, with the proportion of coherent emission approaching unity as the driving strength is reduced [38]. As the population excited within the emitter then becomes very small, it is expected that in solid-state systems the effects of any environmental interactions will correspondingly be suppressed, such that the emitted photon coherence times may become extremely long.

Here, we demonstrate that this intuition is incomplete as phonon interactions remain a vital consideration for QDs in the weak excitation regime, despite the vanishing dot population. Specifically, we show that the sideband resulting from non-Markovian relaxation of the phonon environment is excitation strength independent, unlike the well-studied Markovian phonon contribution [27,28]. It thus leads to an intrinsic subunity limit to the fraction of coherently scattered light from a solid-state emitter, even in the absence of charge fluctuations and no matter how weak the driving. This is in clear contrast to the atomic case, constituting a non-standard regime of semiconductor quantum optics. It is also of direct practical importance, for example, to light-matter coupling schemes that rely on the coherent scattering of photons with high efficiency [39,40]. Furthermore, we show that the impact of the phonon relaxation process can be even more pronounced in two-photon interference experiments, resulting in a substantial suppression of the photon coalescence visibility on picosecond time scales, which is exacerbated when accounting for the inevitable detector temporal response. This leads to a nonmonotonic dependence of the visibility on driving strength that is unexpectedly optimized at intermediate rather than very weak excitation.

Model. We model the QD as a two-level system [27,28,41–43], having an upper (single exciton) state $|X\rangle$ of frequency ω_X and ground state $|0\rangle$, under continuous-wave (cw) excitation with a Rabi frequency Ω and detuning δ. Generalizing to pulsed excitation is possible by introducing a time-dependent Rabi frequency in analogy with Ref. [43]. The electromagnetic and vibrational environments are treated as two separate reservoirs of harmonic oscillators. Within a frame rotating at the laser frequency ω_l, the Hamiltonian may be written ($\hbar = 1$)

$$H = \delta\sigma^\dagger\sigma + \frac{\Omega}{2}\sigma_x + \sum_k \nu_k b_k^\dagger b_k + \sum_m \omega_m a_m^\dagger a_m + \sigma^\dagger\sigma\sum_k g_k(b_k^\dagger + b_k) + \sum_m f_m\sigma^\dagger a_m e^{i\omega_l t} + \text{H.c.}, \tag{1}$$

*jakeilessmith@gmail.com

†ahsan.nazir@manchester.ac.uk

where $\sigma^\dagger = |X\rangle\langle 0|$, $\sigma_x = \sigma^\dagger + \sigma$, and we have applied a rotating-wave approximation to the driving field. Each phonon mode is characterized by a creation (annihilation) operator $b_k^\dagger$ (b_k), frequency ν_k, and couples to the system with strength g_k. Similarly, the electromagnetic environment modes are defined by creation (annihilation) operators $a_m^\dagger$ (a_m), frequencies ω_m, and couplings f_m.

The interactions between the QD and the two harmonic environments are determined by their spectral densities. For the phonon environment, we take the standard form [27,28,44] $J_{\rm PH}(\nu) = \sum_k g_k^2 \delta(\nu - \nu_k) = \alpha \nu^3 \exp(-\nu^2/\nu_c^2)$, where α is the system-environment coupling strength and ν_c is the phonon cutoff frequency, the inverse of which approximately specifies the phonon bath relaxation time scale and is directly related to the ratio of the QD size d and the speed of sound v [44]. The situation is simplified for the electromagnetic environment; for a QD in a bulk medium [45], the local density of states of the electromagnetic field does not vary appreciably over the relevant QD energy scales. This allows us to assume the spectral density to be flat [33,38], $J_{\rm EM}(\omega) = \sum_m |f_m|^2 \delta(\omega - \omega_m) \approx 2\gamma/\pi$, where γ is the spontaneous emission rate.

The dynamics generated by Eq. (1) is not in general amenable to exact solutions. However, in regimes relevant to QD systems we may derive a very accurate master equation (ME) for the reduced state of the QD using the polaron formalism [43,46–48], which is valid beyond the standard limit of weak QD-phonon coupling [43,44]. As we shall see, our treatment, though Markovian in the polaron representation, still retains non-Markovian processes for operators evaluated in the original representation. This makes it particularly well suited to probing different phonon effects in QD optical emission properties, as it allows us to draw a formal connection between the QD dynamics (generated by the ME) and the characteristics of the emitted electromagnetic field via the quantum regression theorem in the usual way, though without imposing restrictions to Markovian or weak-coupling regimes between the QD and phonons [49]. This is especially important in the weak-driving limit, where we shall show that non-Markovian relaxation of the phonon environment has a particularly pronounced effect.

To derive the ME, we apply a polaron transformation to Eq. (1), defined through $H_{\rm P} = \mathcal{U}_{\rm P} H \mathcal{U}_{\rm P}^\dagger$, where $\mathcal{U}_{\rm P} = |0\rangle\langle 0| + |X\rangle\langle X| B_+$, with $B_\pm = \exp[\pm \sum_k g_k (b_k^\dagger - b_k)/\nu_k]$. This removes the linear QD-phonon coupling term, resulting in a transformed Hamiltonian that may be written as $H_{\rm P} = H_{\rm P}^0 + H_{\rm P}^{\rm I}$, with

$$H_{\rm P}^0 = \tilde{\delta}\sigma^\dagger\sigma + \frac{\Omega_r}{2}\sigma_x + \sum_k \nu_k b_k^\dagger b_k + \sum_m \omega_m a_m^\dagger a_m, \quad (2)$$

$$H_{\rm P}^{\rm I} = \frac{\Omega}{2}\sigma^\dagger (B_+ - B) + \sum_m f_m \sigma^\dagger B_+ a_m e^{i\omega_l t} + {\rm H.c.} \quad (3)$$

Here, $\tilde{\delta} = \delta - \sum_k g_k^2/\nu_k$ is the phonon shifted detuning and $\Omega_r = \Omega B$ is the renormalized Rabi frequency, with $B = {\rm tr}(B_\pm \rho_B)$ the average displacement of the phonon environment. For a thermal state of the phonons we have $\rho_B = \exp[-\beta \sum_k \nu_k b_k^\dagger b_k]/\,{\rm tr}_B(\exp[-\beta \sum_k \nu_k b_k^\dagger b_k])$ with temperature $T = (k_B\beta)^{-1}$, and we find $B = \exp[-\frac{1}{2}\int_0^\infty \nu^{-2} J_{\rm PH}(\nu)\coth(\beta\nu/2) d\nu]$. Tracing out the environments within the Born-Markov approximations [50], we obtain a polaron frame ME that is second order in $H_{\rm P}^{\rm I}$ but nonperturbative in the original QD-phonon coupling. For $\tilde{\delta} = 0$ the ME can be written [51]

$$\dot{\rho}_{\rm P}(t) = -\frac{i\Omega_r}{2}[\sigma_x, \rho_{\rm P}(t)] + \mathcal{K}_{\rm PH}[\rho_{\rm P}(t)] + \mathcal{K}_{\rm EM}[\rho_{\rm P}(t)], \quad (4)$$

where $\mathcal{K}_{\rm EM}[\rho_{\rm P}(t)] = \frac{\gamma}{2}[2\sigma\rho_{\rm P}(t)\sigma^\dagger - \{\sigma^\dagger\sigma, \rho_{\rm P}(t)\}]$ arises from the second term in Eq. (3) and describes spontaneous emission, with $\rho_{\rm P}$ the polaron frame reduced QD density operator. Markovian dissipative processes due to phonons are encoded in the superoperator $\mathcal{K}_{\rm PH}[\rho_{\rm P}(t)]$ which originates from the first term in Eq. (3) [51]. Though the form of $\mathcal{K}_{\rm PH}[\rho_{\rm P}(t)]$ can in general be rather complicated, it is evident that the influence of these *Markovian* phonon terms becomes negligible as $\Omega/\gamma \to 0$ and the weak-driving (Heitler) regime is approached, in line with conventional expectations.

Photon emission. We shall now see how the polaron formalism also allows for non-Markovian phonon processes to be readily included into the emitted field characteristics. Crucially, we shall find that this influence *does not* disappear as $\Omega/\gamma \to 0$, unlike the standard Markovian one. We consider the electric field operator in the Heisenberg picture, which, neglecting polarization, may be written $\hat{\boldsymbol{E}}(t) = \hat{\boldsymbol{E}}^{(+)}(t) + \hat{\boldsymbol{E}}^{(-)}(t)$, with a positive frequency component $\hat{\boldsymbol{E}}^{(+)}(t) = [\hat{\boldsymbol{E}}^{(-)}(t)]^\dagger = \sum_m \mathcal{E}_m \hat{a}_m(t)$, where $\mathcal{E}_m$ is the electric field strength. Using the formal solution of the Heisenberg equation for $a_m(t)$, we may write $\hat{E}^{(+)}(t) = -i\sum_m \int_0^t dt' \mathcal{E}_m f_m \tilde{\sigma}(t') B_-(t') e^{i\omega_m(t'-t)}$, where $\tilde{\sigma}(t) = \sigma(t)e^{-i\omega_l t}$, and we have omitted the free field contribution $\sum_m \mathcal{E}_m \hat{a}_m(0) e^{-i\omega_m t}$, valid when taking expectation values assuming a free field in the vacuum state. Using, as before, the fact that the coupling between the emitter and field does not vary appreciably over energy scales relevant to the QD, we then obtain

$$\hat{E}^{(+)}(t) \to -i\mathcal{E}\sqrt{\frac{\pi\gamma}{2}}\tilde{\sigma}(t) B_-(t), \quad (5)$$

which we see contains the phonon displacement operator $B_-(t)$. This results from the transformation to the polaron frame, and captures the relaxation of the vibrational environment when a photon is scattered. This is an inherently non-Markovian process, occurring on a time scale set by $1/\nu_c \propto d/v \sim 1$ ps [49]. Interestingly, such non-Markovian effects are not evident in the QD populations, studied, e.g., in Ref. [43], as the relevant operators commute with the polaron transformation.

The impact of the phonon relaxation process can be observed, however, in the steady-state intensity spectrum of light emitted from the QD, where its picosecond time scale translates to a broad meV-scale feature. The spectrum is related to the field operators through the Wiener-Khinchin theorem, $S(\omega) = \lim_{t\to\infty} {\rm Re}[\int_0^\infty \langle \hat{E}^{(-)}(t)\hat{E}^{(+)}(t+\tau)\rangle e^{i(\omega-\omega_l)\tau} d\tau]$ [38]. Using Eq. (5) we find $S(\omega) \propto {\rm Re}[\int_0^\infty g^{(1)}(\tau) e^{i(\omega-\omega_l)\tau} d\tau]$, with $g^{(1)}(\tau) = \lim_{t\to\infty}\langle \sigma^\dagger(t) B_+(t) \sigma(t+\tau) B_-(t+\tau)\rangle$ [52–54]. The level of coherent scattering is determined by the long-time limit of the correlation function, $g^{(1)}_{\rm coh} = \lim_{\tau\to\infty}[g^{(1)}(\tau)]$, and the incoherent emission

RAPID COMMUNICATIONS

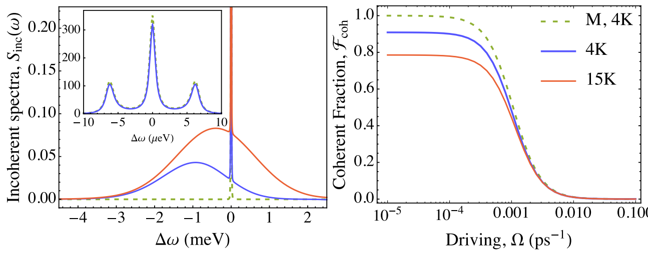

FIG. 1. Left: Incoherent emission spectrum for a cw-driven QD, demonstrating the presence of the broad phonon sideband captured by the non-Markovian theory (solid), when compared to the Markovian expression (dashed). The inset shows a zoom around the QD resonance at 4 K. Right: Fraction of coherent scattering as a function of driving strength within the non-Markovian theory (solid) and the Markovian approximation (M, dashed). Parameters: $\Omega = 0.01$ ps^{-1}, $\gamma^{-1} = 700$ ps, with the phonon environment characterized by $\alpha = 0.03$ ps^2, $\omega_c = 2.2$ ps^{-1}, and temperatures as indicated.

spectrum as $S_{\rm inc}(\omega) = {\rm Re}\,[\int_0^\infty [g^{(1)}(\tau) - g^{(1)}_{\rm coh}]e^{i(\omega-\omega_l)\tau} d\tau]$. For typical QD systems, $g^{(1)}(\tau)$ contains two quite distinct time scales: the aforementioned picosecond time scale associated with phonon relaxation, and a much longer (∼ns) time scale corresponding to photon emission. This allows us to factorize the correlation function into short- and long-time contributions, such that $g^{(1)}(\tau) = G(-\tau)g_0^{(1)}(\tau)$, where $g_0^{(1)}(\tau) = \lim_{t\to\infty}\langle\sigma^\dagger(t)\sigma(t+\tau)\rangle$ can be calculated from Eq. (4) using the (Markovian) regression theorem, while $G(\tau) = \langle B_+(\tau)B_-\rangle = B^2 \exp[\int_0^\infty \nu^{-2} J_{\rm PH}(\nu)[\coth(\beta\nu/2)\cos\nu\tau - i\sin\nu\tau]d\nu]$ describes short-time phonon bath relaxation.

Spectra. The impact of these non-Markovian phonon processes is illustrated in Fig. 1 (left), where we plot the incoherent spectrum including (solid lines) and excluding (dashed lines) the short-time phonon contribution $G(\tau)$. The inset shows a zoom around $\Delta\omega = \omega - \omega_l = 0$, where both approaches capture the Mollow triplet, while only the non-Markovian theory captures the broad sideband visible on the scale of the main plot. Such sidebands have been observed in resonance fluorescence experiments on QDs [13–16], and previously studied theoretically using a non-Markovian regression theorem [49]. Not only does our approach provide a simple method for capturing these contributions (i.e., one that does not rely on non-Markovian extensions to the regression theorem), but it also allows us to easily separate the phonon sideband and direct emission into independent contributions, since $S(\omega) = {\rm Re}\,[\int_0^\infty [G(-\tau) - B^2]g_0^{(1)}(\tau)e^{-i(\omega-\omega_l)\tau}d\tau] + B^2\,{\rm Re}\,[\int_0^\infty g_0^{(1)}(\tau)e^{-i(\omega-\omega_l)\tau}d\tau]$. Here, the first term corresponds to the sideband emission, and we make use of the fact that $G(-\tau) \to B^2$ after approximately 1 ps, on which time scale $g_0^{(1)}(\tau)$ is almost static. Integrating the spectrum over all frequencies we find that the fraction of power emitted via the phonon sideband is given by $(1 - B^2)$. Thus, even at $T = 0$ the sideband constitutes $(1 - B^2) \approx 7\%$ of the total emission, rising to 9.1% at $T = 4$ K and 22.5% at $T = 15$ K, consistent with experimental observations [14,15]. In the time domain the sideband corresponds to a rapid (ps) decrease of the $g^{(1)}$ fringe visibility to $B^2 \approx 90.9\%$ at 4 K, which is also in accord with experiments performed in the Heitler limit [16].

Our formalism also reveals important physics. It is apparent from the expression for $g^{(1)}(\tau)$ that the fraction of light emitted through the phonon sideband is independent of the laser excitation conditions. This has particularly significant implications at weak driving, where it affects the balance of coherent and incoherent emission. For atomic or Markovian systems under very weak excitation, light incident on the emitter scatters predominantly elastically, maintaining phase coherence with the driving field. However, we now see that for QDs, when accounting for non-Markovian phonon bath relaxation, some fraction of the light is *always* emitted incoherently through the sideband regardless of the driving strength. Hence, the fraction of coherently scattered light is reduced below unity at weak driving, as can be seen in Fig. 1 (right), leading to an intrinsic limit to the level of coherent scattering from such a solid-state photonic system that worsens as temperature is raised. Although we have formulated our treatment for the case of cw excitation, the independence of the sideband contribution on driving conditions implies that it will also be present for pulsed excitation, which is consistent with experiment, too [15].

Though the limit to coherent scattering could be overcome by filtering out the sideband, in this case, the non-Markovian phonon relaxation process still imposes an intrinsic operational limitation as it leads now to a loss in efficiency of $1 - B^2$. A trade-off then exists between the level of coherent scattering and the source efficiency. This reduction in efficiency may to some extent be mitigated by Purcell enhancement for a QD coupled to a narrow cavity mode [55], though this too cannot be done arbitrarily, as the cavity can only enhance the B^2 fraction of light falling within its linewidth.

Two-photon coalescence. Given that phonon relaxation acts to reduce first-order coherence, it is natural to ask whether it also affects the visibility of two-photon interference as measured in a Hong-Ou-Mandel (HOM) experiment. We consider the steady-state intensity correlation function $g^{(2)}(\tau) = \lim_{t\to\infty}\langle\hat{E}_3^-(t)\hat{E}_4^-(t+\tau)\hat{E}_4^+(t+\tau)\hat{E}_3^+(t)\rangle/(\langle\hat{E}_3^-\hat{E}_3^+\rangle\langle\hat{E}_4^-\hat{E}_4^+\rangle)$ as measured by an unbalanced Mach-Zehnder interferometer, with detected output fields $\hat{E}_3(t)$ and $\hat{E}_4(t)$. We calculate $g^{(2)}(\tau)$ in the same manner as the first-order correlation function, where phonon operators enter again via Eq. (5) [51].

In contrast to two-photon interference experiments using pulsed excitation, for cw systems the time resolution of the photon detectors becomes an important consideration [19]. For example, for an ideal detector with perfect time resolution, complete coalescence $[g^{(2)}(0) = 0]$ may be observed at zero time delay regardless of the spectral indistinguishability of the incident photons [56–58], the detectors being unable to distinguish frequency or phase differences between the two. However, the more distinguishable the photons are, the smaller the time window over which $g^{(2)}(\tau) \approx 0$ [19]. As such, photon detectors with realistic response times will not resolve two-photon interference for sufficiently distinguishable photons.

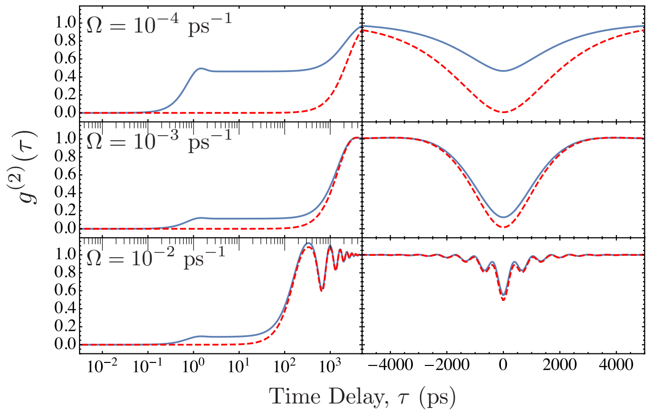

FIG. 2. HOM second-order correlation function before (left, log scale) and post (right) detector convolution, including (solid) and without (dashed) non-Markovian phonon relaxation processes. At weak excitation, the convolved HOM dip is significantly shallower when including non-Markovian relaxation. Parameters: As Fig. 1 with $T = 4$ K.

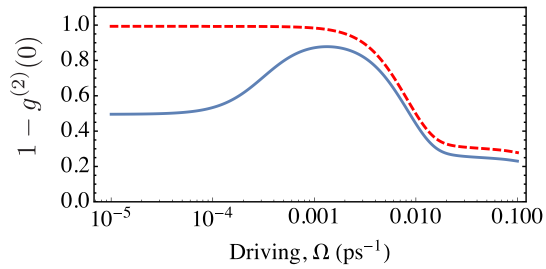

FIG. 3. HOM-dip depth post detector convolution as a function of driving strength for the Markovian (dashed) and non-Markovian (solid) theories. Parameters as in Fig. 2.

The influence of phonon bath relaxation on two-photon coalescence is seen in Fig. 2 (left), where we plot $g^{(2)}(\tau)$ below saturation ($s = \sqrt{2}\Omega/\gamma \approx 0.1$, top), at saturation ($s \approx 1$, middle), and above ($s \approx 10$, bottom), assuming perfect detectors. Phonon bath relaxation manifests as a sharp short-time feature around $\tau = 0$, clearly apparent in the non-Markovian theory (solid curves), and particularly pronounced at weak excitation. In contrast, the Markovian theory (dashed curves) predicts much slower dynamics at weak-driving strengths, a consequence of the vanishing phonon influence within this approach. To account for nonideal detectors, we convolve the correlation function with a Gaussian response function $R(x) = (2/\delta\tau)\sqrt{\log 2/\pi}\exp[-4\log 2x^2/\delta\tau^2]$ of full width at half maximum $\delta\tau = 400$ ps [59]. This gives the intensity correlation function as measured in a realistic experiment, and the result is shown in Fig. 2 (right). We see that the convolution washes out the detailed features associated to phonon bath relaxation as the detectors are unable to resolve the dip at zero time delay, reducing the effective visibility of two-photon interference.

This is highlighted by Fig. 3, where the measured dip depth postconvolution is shown as a function of driving strength. At weak driving (below saturation), the Markovian theory predicts perfect interference as the photons are then unaffected by phonons, and share the same coherence properties as the driving field. Accounting for phonon relaxation, however, the coalescence visibility drops dramatically to $1 - g^{(2)}(0) \approx 0.5$. This reduction occurs due to the long-time scale associated with optical scattering processes in the weak-driving limit, which allows the phonon environment to relax fully between scattering events. As the driving strength is increased, so too is the rate at which photons are scattered, and thus the visibility improves. Above saturation ($s \approx 10$ for $\Omega \sim 10^{-2}$ ps^{-1}), the correlation function develops Rabi oscillations, which cannot be fully resolved by the detector when $\delta\tau \sim \Omega^{-1}$, resulting in a drop in visibility.

An important implication of these results is that for cw-driven solid-state emitters with realistic detectors, the weak excitation regime is not optimal for generating indistinguishable photons. Instead, this lies near the onset of strong driving (i.e., around saturation), where in fact the level of incoherent scattering can be larger than the coherent contribution. This is in marked contrast to atomic systems, where increasing the fraction of coherent scattering always improves the visibility. We note that two-photon interference has been observed experimentally with QDs from below to above saturation [17,19,20], thus our predictions should be testable using unfiltered emission.

Summary. We have shown that non-Markovian phonon bath relaxation processes in driven QDs are excitation strength independent. They thus have a profound impact on the level of coherently and incoherently scattered light, limiting the coherent fraction to values of ≈90% at $T = 4$ K. Moreover, when accounting for any realistic detector response time, these short-time phonon relaxation processes act to decrease two-photon HOM interference visibilities. These results have important implications for numerous quantum technology applications where an efficient source of coherently scattered photons is needed as a resource [39,40]. We stress that although our calculations have been formulated in the context of QDs, the results are expected to be applicable to a variety of solid-state emitters, including nitrogen vacancy centers [60], superconducting qubits, and dye molecules embedded in crystalline lattices [61,62].

Acknowledgments. J.I.-S. and J.M. acknowledge support from the Danish Research Council (DFF-4181-00416) and Villum Fonden (NATEC Centre). A.N. is supported by University of Manchester and the Engineering and Physical Sciences Research Council. This project has received funding from the European Union's Horizon 2020 research and innovation programme under the Marie Sklodowska-Curie grant agreement No. 703193.

[1] M. Bayer, O. Stern, P. Hawrylak, S. Fafard, and A. Forchel, Nature (London) **405**, 923 (2000).

[2] C. Santori, D. Fattal, J. Vuckovic, G. S. Solomon, and Y. Yamamoto, Nature (Londond) **419**, 594 (2002).

[3] K. Brunner, U. Bockelmann, G. Abstreiter, M. Walther, G. Böhm, G. Tränkle, and G. Weimann, Phys. Rev. Lett. **69**, 3216 (1992).
[4] D. Press, S. Götzinger, S. Reitzenstein, C. Hofmann, A. Löffler, M. Kamp, A. Forchel, and Y. Yamamoto, Phys. Rev. Lett. **98**, 117402 (2007).
[5] O. Fedorych, C. Kruse, A. Ruban, D. Hommel, G. Bacher, and T. Kümmell, Appl. Phys. Lett. **100**, 061114 (2012).
[6] E. B. Flagg, A. Muller, S. V. Polyakov, A. Ling, A. Migdall, and G. S. Solomon, Phys. Rev. Lett. **104**, 137401 (2010).
[7] M. Müller, S. Bounouar, K. D. Jöns, M. Glässl, and P. Michler, Nat. Photonics **8**, 224 (2014).
[8] R. M. Stevenson, R. J. Young, P. Atkinson, K. Cooper, D. A. Ritchie, and A. J. Shields, Nature (London) **439**, 179 (2006).
[9] E. B. Flagg, A. Muller, J. W. Robertson, S. Founta, D. G. Deppe, M. Xiao, W. Ma, G. J. Salamo, and C. K. Shih, Nat. Phys. **5**, 203 (2009).
[10] L. Monniello, C. Tonin, R. Hostein, A. Lemaitre, A. Martinez, V. Voliotis, and R. Grousson, Phys. Rev. Lett. **111**, 026403 (2013).
[11] S. Ates, S. M. Ulrich, S. Reitzenstein, A. Löffler, A. Forchel, and P. Michler, Phys. Rev. Lett. **103**, 167402 (2009).
[12] S. M. Ulrich, S. Ates, S. Reitzenstein, A. Löffler, A. Forchel, and P. Michler, Phys. Rev. Lett. **106**, 247402 (2011).
[13] K. Konthasinghe, J. Walker, M. Peiris, C. K. Shih, Y. Yu, M. F. Li, J. F. He, L. J. Wang, H. Q. Ni, Z. C. Niu, and A. Muller, Phys. Rev. B **85**, 235315 (2012).
[14] C. Matthiesen, M. Geller, C. H. H. Schulte, C. Le Gall, J. Hansom, Z. Li, M. Hugues, E. Clarke, and M. Atatüre, Nat. Commun. **4**, 1600 (2013).
[15] A. C. Dada, T. S. Santana, R. N. E. Malein, A. Koutroumanis, Y. Ma, J. M. Zajac, J. Y. Lim, J. D. Song, and B. D. Gerardot, Optica **3**, 493 (2016).
[16] C. Matthiesen, A. N. Vamivakas, and M. Atatüre, Phys. Rev. Lett. **108**, 093602 (2012).
[17] R. N. E. Malein, T. S. Santana, J. M. Zajac, A. C. Dada, E. M. Gauger, P. M. Petroff, J. Y. Lim, J. D. Song, and B. D. Gerardot, Phys. Rev. Lett. **116**, 257401 (2016).
[18] C. H. H. Schulte, J. Hansom, A. E. Jones, C. Matthiesen, C. Le Gall, and M. Atatüre, Nature (London) **525**, 222 (2015).
[19] R. Proux, M. Maragkou, E. Baudin, C. Voisin, P. Roussignol, and C. Diederichs, Phys. Rev. Lett. **114**, 067401 (2015).
[20] S. Kalliakos, Y. Brody, A. J. Bennett, D. J. P. Ellis, J. Skiba-Szymanska, I. Farrer, J. P. Griffiths, D. A. Ritchie, and A. J. Shields, Appl. Phys. Lett. **109**, 151112 (2016).
[21] O. Gazzano *et al.*, Nat. Commun. **4**, 1425 (2013).
[22] X. Ding, Y. He, Z. C. Duan, N. Gregersen, M. C. Chen, S. Unsleber, S. Maier, C. Schneider, M. Kamp, S. Höfling, C.-Y. Lu, and J.-W. Pan, Phys. Rev. Lett. **116**, 020401 (2016).
[23] N. Somaschi, V. Giesz, L. De Santis, J. C. Loredo, M. P. Almeida, G. Hornecker, S. L. Portalupi, T. Grange, C. Anton, J. Demory, C. Gomez, I. Sagnes, N. D. L. Kimura, A. Lemaitre, A. Auffeves, A. G. White, L. Lanco, and P. Senellart, Nat. Photonics **10**, 340 (2016).
[24] A. Thoma, P. Schnauber, M. Gschrey, M. Seifried, J. Wolters, J. H. Schulze, A. Strittmatter, S. Rodt, A. Carmele, A. Knorr, T. Heindel, and S. Reitzenstein, Phys. Rev. Lett. **116**, 033601 (2016).
[25] P. Lodahl, S. Mahmoodian, and S. Stobbe, Rev. Mod. Phys. **87**, 347 (2015).
[26] N. Gregersen, P. Kaer, and J. Mørk, IEEE J. Sel. Top. Quantum Electron. **19**, 9000516 (2013).
[27] A. J. Ramsay, A. V. Gopal, E. M. Gauger, A. Nazir, B. W. Lovett, A. M. Fox, and M. S. Skolnick, Phys. Rev. Lett. **104**, 017402 (2010).
[28] A. J. Ramsay, T. M. Godden, S. J. Boyle, E. M. Gauger, A. Nazir, B. W. Lovett, A. M. Fox, and M. S. Skolnick, Phys. Rev. Lett. **105**, 177402 (2010).
[29] P. Kaer, P. Lodahl, A.-P. Jauho, and J. Mørk, Phys. Rev. B **87**, 081308 (2013).
[30] J. Houel, A. V. Kuhlmann, L. Greuter, F. Xue, M. Poggio, B. D. Gerardot, P. A. Dalgarno, A. Badolato, P. M. Petroff, A. Ludwig, D. Reuter, A. D. Wieck, and R. J. Warburton, Phys. Rev. Lett. **108**, 107401 (2012).
[31] A. V. Kuhlmann, J. Houel, A. Ludwig, L. Greuter, D. Reuter, A. D. Wieck, M. Poggio, and R. J. Warburton, Nat. Phys. **9**, 570 (2013).
[32] A. V. Kuhlmann, J. H. Prechtel, J. Houel, A. Ludwig, D. Reuter, A. D. Wieck, and R. J. Warburton, Nat. Commun. **6**, 8204 (2015).
[33] D. P. S. McCutcheon and A. Nazir, Phys. Rev. Lett. **110**, 217401 (2013).
[34] J. Iles-Smith and A. Nazir, Optica **3**, 207 (2016).
[35] S. Hughes and H. J. Carmichael, New J. Phys. **15**, 053039 (2013).
[36] J. H. Quilter, A. J. Brash, F. Liu, M. Glässl, A. M. Barth, V. M. Axt, A. J. Ramsay, M. S. Skolnick, and A. M. Fox, Phys. Rev. Lett. **114**, 137401 (2015).
[37] P. Kaer and J. Mørk, Phys. Rev. B **90**, 035312 (2014).
[38] H. Carmichael, *Statistical Methods in Quantum Optics 1: Master Equations and Fokker-Planck Equations* (Springer, Berlin, 1998).
[39] C. Y. Hu, A. Young, J. L. O'Brien, W. J. Munro, and J. G. Rarity, Phys. Rev. B **78**, 085307 (2008).
[40] C. Y. Hu and J. G. Rarity, Phys. Rev. B **91**, 075304 (2015).
[41] D. Bimberg, M. Grundmann, and N. N. Ledentsov, *Quantum Dot Heterostructures* (Wiley, Hoboken, NJ, 1999).
[42] A. Zrenner, E. Beham, S. Stufler, F. Findeis, M. Bichler, and G. Abstreiter, Nature (London) **418**, 612 (2002).
[43] D. P. S. McCutcheon and A. Nazir, New J. Phys. **12**, 113042 (2010).
[44] A. Nazir, Phys. Rev. B **78**, 153309 (2008).
[45] Or, for example, a QD placed in the center of a photonic crystal waveguide within the Purcell regime.
[46] Y.-J. Wei, Y. He, Y.-M. He, C.-Y. Lu, J.-W. Pan, C. Schneider, M. Kamp, S. Höfling, D. P. S. McCutcheon, and A. Nazir, Phys. Rev. Lett. **113**, 097401 (2014).
[47] C. Roy and S. Hughes, Phys. Rev. X **1**, 021009 (2011).
[48] A. Nazir and D. P. S. McCutcheon, J. Phys.: Condens. Matter **28**, 103002 (2016).
[49] D. P. S. McCutcheon, Phys. Rev. A **93**, 022119 (2016).
[50] H. P. Breuer and F. Petruccione, *The Theory of Open Quantum Systems* (Oxford University Press, Oxford, UK, 2002).
[51] See Supplemental Material at http://link.aps.org/supplemental/10.1103/PhysRevB.95.201305 for additional details on the background theory and derivations.
[52] K. Roy-Choudhury and S. Hughes, Opt. Lett. **40**, 1838 (2015).
[53] K. Roy-Choudhury and S. Hughes, Phys. Rev. B **92**, 205406 (2015).
[54] K. Roy-Choudhury and S. Hughes, Optica **2**, 434 (2015).

[55] T. Grange, G. Hornecker, D. Hunger, J.-P. Poizat, J.-M. Gérard, P. Senellart, and A. Auffèves, Phys. Rev. Lett. **114**, 193601 (2015).
[56] J. Metz and S. D. Barrett, Phys. Rev. A **77**, 042323 (2008).
[57] T. Legero, T. Wilk, M. Hennrich, G. Rempe, and A. Kuhn, Phys. Rev. Lett. **93**, 070503 (2004).
[58] T. Legero, T. Wilk, A. Kuhn, and G. Rempe, Appl. Phys. B **77**, 797 (2003).
[59] R. B. Patel, A. J. Bennett, K. Cooper, P. Atkinson, C. A. Nicoll, D. A. Ritchie, and A. J. Shields, Phys. Rev. Lett. **100**, 207405 (2008).
[60] C. Kurtsiefer, S. Mayer, P. Zarda, and H. Weinfurter, Phys. Rev. Lett. **85**, 290 (2000).
[61] J. Hwang and E. A. Hinds, New J. Phys. **13**, 085009 (2011).
[62] C. Polisseni, K. D. Major, S. Boissier, S. Grandi, A. S. Clark, and E. A. Hinds, Opt. Express **24**, 5615 (2016).